

Probing a Steep EoS for Dark Energy with latest observations

Mariana Jaber and Axel de la Macorra

*Instituto de Fisica, Universidad Nacional Autonoma de Mexico,
A.P. 20-364, 01000, Mexico D.F., Mexico*

We present a parametrization for the Dark Energy Equation of State “EoS” which has a rich structure, performing a transition at pivotal redshift z_T between the present day value w_0 to an early time $w_i = w_a + w_0 \equiv w(z \gg 0)$ with a steepness given in terms of q parameter. The proposed parametrization is $w = w_0 + w_a(z/z_T)^q/(1 + (z/z_T))^q$, with w_0, w_i, q and z_T constant parameters. It reduces to the widely used EoS $w = w_0 + w_a(1 - a)$ for $z_T = q = 1$. This transition is motivated by scalar field dynamics such as for example quintessence models. We study if a late time transition is favored by BAO measurements combined with local determination of H_0 and information from the CMB. According to our results, an EoS with a present value of $w_0 = -0.92$ and a high redshift value $w_i = -0.99$, featuring a transition at $z_T = 0.28$ with an exponent $q = 9.97$ was favored by data coming from local dynamics of the Universe (BAO combined with H_0 determination). We find that a dynamical DE model allows to simultaneously fit H_0 from local determinations and Planck CMB measurements, alleviating the tension obtained in a Λ CDM model. Additionally to this analysis we solved numerically the evolution of matter over-densities in the presence of dark energy both at background level and when its perturbations were considered. We show that the presence of a steep transition in the DE EoS gets imprinted into the evolution of matter overdensities and that the addition of an effective sound speed term does not erase such feature.

I. INTRODUCTION

We live in a particular epoch of the cosmic history characterized by the acceleration in the expansion rate of the Universe. Although its cause is unknown this acceleration is described as the consequence of a Cosmological Constant, Λ , with density ρ_Λ constant in space and time. Despite its simplicity, there is no fundamental understanding of its origin and this framework has serious theoretical issues namely the coincidence and fine-tuning problems([1, 2]). For this reason alternative models that either modify gravity at large scales as prescribed by General Relativity or introduce a dynamical Dark Energy (DE) component have arisen. Dynamical dark energy models are often characterized by the DE equation of state (EoS), $w \equiv P/\rho$, which is the ratio of the DE pressure to its density. Since DE properties are still unknown, several models to parametrize its EoS as a function of time, $w(z)$, have arisen in the literature ([3–13]). One of the most popular among them is the CPL parametrization ([14],[15]), widely used in cosmological observational analysis. The present value of DE EoS is restricted by observations to be close to -1 ($w = -1.019^{+0.075}_{-0.080}$ according to the 95% limits imposed by *Planck* data combined with other astrophysical measurements [16]). Nevertheless, the DE behavior and its properties at different cosmic epochs are much poorly constrained by current cosmological observations. According to astrophysical observations our Universe is flat and dominated at present time by the DE component ([16]), so data coming from late-time, low-redshift measurements such as Baryon Acoustic Oscillations

(BAO) from Large Scale Structure surveys are those best suited for its analysis.

The aim of this work is to determine the late time dynamics of DE through its EoS, and in particular we are interested in studying if a transition in $w(z)$ takes place. To that end the parametrization used is $w(z) = w_0 + w_a(z/z_T)^q/[1 + (z/z_T)]^q$, with $w_0, w_a = w_i - w_0, q$, and z_T constant parameters. This EoS allows for a steep transition for a large value of q at the pivotal point z_T , which is prompted by scalar field dynamics such as quintessence models [17] and motivated in [13], where a new parametrization that captures the dynamics of DE is presented.

The scientific community is devoting a large amount of time and resources in the quest to understand the dynamics and nature of DE, working on current (SDSS-IV [18], DES [19]) and future (DESI [20–22], Euclid [23], LSST [24]) experiments to study with very high precision the expansion history of the Universe and thus be able to test interesting models beyond a Cosmological Constant or Taylor expansions of the EoS of DE.

This article is organized as follows: we introduce our theoretical framework and the data sets used in Section II, Section III details the analysis performed at Background level and the results obtained, Section IV discusses the analysis at perturbative level while Section V summarizes our Conclusions.

II. METHOD AND DATA

Within the General Relativity framework for a flat Universe and a FLRW metric we have

$$H(z) = H_0 \sqrt{\Omega_r(1+z)^4 + \Omega_m(1+z)^3 + \Omega_{DE}F(z)} \quad (1)$$

where $H \equiv (\frac{da}{dt})(\frac{1}{a})$ is the Hubble parameter, $a = (1+z)^{-1}$ the scale factor of the Universe and $H_0 = 100 \cdot h$ is the Hubble parameter at redshift zero in units of $km \cdot s^{-1} Mpc^{-1}$. The present value of matter, radiation, and DE fractional densities are given by Ω_m , Ω_r , Ω_{DE} , respectively. The function $F(z) \equiv \frac{\rho_{DE}(z)}{\rho_{DE}(0)}$ in equation (1) encodes the evolution of DE component in terms of its EoS, $w(z)$, according to

$$F(z) = \exp\left(-3 \int_0^z dz' \frac{1+w(z')}{1+z'}\right) \quad (2)$$

where $w(z)$ specifies the evolution of the DE fluid and accordingly, the Universe expansion rate at late times, following the dynamics set by equation (1).

$$w(z) = w_0 + w_a \frac{(\frac{z}{z_T})^q}{1 + (\frac{z}{z_T})^q} \quad (3)$$

with $w_a = w_i - w_0$ where w_i and w_0 represent the value for $w(z)$ at large redshifts and at present day, respectively, whereas the term $f(z) \equiv \frac{(\frac{z}{z_T})^q}{1 + (\frac{z}{z_T})^q}$ modulates the dynamics of this parametrization in between both values, and takes the values $f(z=0) = 0$, $f(z \rightarrow \infty) = 1$ and $f(z=z_T) = 1/2$, *i.e.* $0 \leq f(z) \leq 1$. This EoS makes a transition between the two regimes: $w(z=0) \rightarrow w_0$, $w(z \gg 0) \rightarrow w_i$, at redshift $z = z_T$, taking a value of $w(z_T) = (w_0 + w_i)/2$. The parameter q modulates the steepness of the transition featured: a larger value for q has a steeper transition, as figure 1 shows.

For $q = z_T = 1$, equation (3) includes the well known CPL parametrization ([14, 15]) as a particular case but it allows for a richer physical behavior. CPL EoS written in terms of scale factor reads:

$$w(a) = w_0 + w_a(1-a) \quad (4)$$

from where we see that its slope is constant and with a value $dw(a)/da = -w_a = -(w_i - w_0)$, meaning that the late time dynamics of DE is fixed from the present and initial values of the EoS.

Clearly, taking $w_0 = w_i = -1$ in (3), the Cosmological Constant solution, $w_\Lambda \equiv -1$, is recovered.

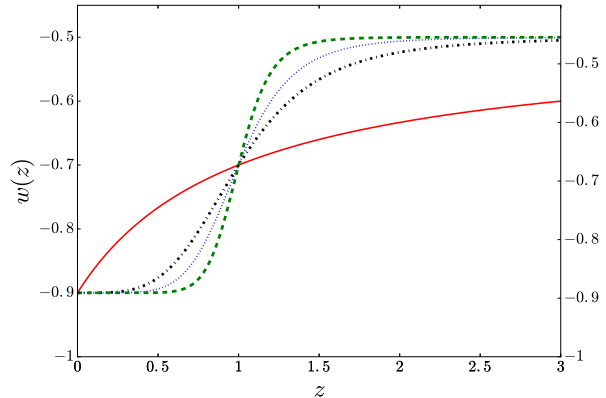


FIG. 1: Evolution of $w(z)$ from equation (3) with $q = 1$ (solid red), $q = 4$ (black dot-dashed), $q = 6$ (blue dotted), and $q = 10$ (green dashed). The other parameters were fixed to $w_0 = -0.9$, $w_i = -0.5$ and $z_T = 1$. The solid red curve takes the special case $q = z_T = 1$, representing the CPL parametrization (4).

A. BAO as a cosmological probe

Ever since its first detection (Cole et al. 2005 [25], Eisenstein et al 2005, [26]) the Baryon Acoustic Oscillation feature has been widely used as a powerful tool for cosmology becoming the standard ruler of choice. It has become the best way to probe late time dynamics of the Universe and in consequence that of DE. For that reason it is the cosmological tool used by several experiments like 6dF [27], WiggleZ [28], SDSS-III [29], (and most recently [30]), SDSS-IV [18] and Dark Energy Survey (DES) [19] and the main probe to be implemented in future experiments like the Dark Energy Spectroscopic Instrument (DESI) [20–22] and Euclid [23].

The corresponding size, $r_{BAO}(z)$, is obtained by performing a spherical average of the galaxy distribution both along and across the line of sight (Bassett and Hlozek 2010 [31]):

$$r_{BAO}(z) \equiv \frac{r_s(z_d)}{D_V(z)} \quad (5)$$

The comoving sound horizon at the baryon drag epoch is represented by $r_s(z_d)$ and the dilation scale, $D_V(z)$, contains information about the cosmology used in $H(z)$:

$$r_s(z_d) \equiv \int_{z_d}^{\infty} \frac{dz}{H(z)\sqrt{3(R(z)+1)}}, \quad (6)$$

$$D_V(z) \equiv \left[\frac{z(1+z)^2}{H(z)} D_A(z)^2 \right]^{1/3}, \quad (7)$$

where

$$D_A(z) = \frac{1}{1+z} \int_0^z \frac{dz'}{H(z')} \quad (8)$$

In this way, the BAO standard ruler which is set by a particular size in the spatial distribution of matter, can be used to constrain the parameters in equation (3).

While the sound horizon, $r_s(z_d)$, depends upon the physics prior to the recombination era, given by $z_d \approx 1059$ [16] and the baryon to photon ratio, $R(z) \equiv \frac{3\Omega_b(z)}{4\Omega_\gamma(z)}$, the dilation scale, $D_V(z)$, is sensitive to the physics of much lower redshifts, particularly to those probed by Large Scale Structure experiments.

In this work we make use of the observational points from the six-degree-field galaxy survey (6dFGS [27]), Sloan Digital Sky Survey Data Release 7 (SDSS DR7 [32]) and the reconstructed value (SDSS(R) [33]), as well as the latest result from the complete BOSS sample SDSS DR12 ([30]), and the Lyman- α Forest (Ly α -F) measurements from the Baryon Oscillation Spectroscopic Data Release 11 (BOSS DR11 [34], [35]). Table I summarizes them all. Since the volume surveyed by BOSS and WiggleZ [28] partially overlap we do not use data from the latter in this work (see details in [36]).

B. Local value of the Hubble Constant

The present value of Hubble constant has been determined observationally from direct measurement of the local dynamics, as in the latest work of A. Riess *et al* in [37], but also from BAO measurements either from galaxy surveys or from the Lyman- α forest and it can be derived as well from CMB experiments such as Planck.

Regarding the work of A. Riess *et al* (AR16), their best estimate in units of $km \cdot s^{-1} Mpc^{-1}$ reports a value of

$$H_0 = 73.21 \pm 1.74, \quad (9)$$

the accuracy of which was achieved in great deal due to the utilization of maser system in NGC1258 both to calibrate and as an independent anchor for the cosmic distance ladder.

C. Cosmic Microwave Background

The Cosmic Microwave Background is the most precise cosmological data set. The angle subtended by the first peak is determined with exquisite precision ([16]):

$$\theta_* = 1.04077 \pm 0.00032 \times 10^{-2} \quad (10)$$

Following the latest report of the Planck collaboration (P15) [38] and [39] we use *Planck TT+TE+EE+lowP* which denotes the combination of likelihood at $l \leq 30$ using TT, TE, and EE spectra with the low- l temperature+polarization likelihood.

However, it has been shown ([40], [41], [38]) that the information of CMB power spectra can be compressed within few observables such as the angular scale of sound horizon at last scattering, $l_A \equiv \pi/\theta_*$, and the scaled distance to last scattering surface, $R \equiv \sqrt{\Omega_M H_0^2} d_A(z_*)$.

We keep the flat geometry and the baryon density fixed and thus we can add the CMB information to BAO and H_0 measurements by means of the observables $\{\theta_*, \omega_c \equiv \Omega_c h^2\}$. The corresponding covariance matrix is

$$\mathcal{C}_{CMB} = \begin{matrix} & \omega_c & \theta_* \\ \omega_c & \begin{pmatrix} -23.5248 & -2.2078 \\ -2.207815 & 1.063561 \end{pmatrix} \end{matrix} \times 10^{-7} \quad (11)$$

The angle of horizon at last scattering is defined to be

$$\theta_* \equiv \frac{r_s(z_*)}{d_A(z_*)} \quad (12)$$

where $r_s(z_*)$ is the horizon size at the decoupling epoch ($z_* \approx 1090.06$ according to Planck [16]), defined by the integral in equation (6) evaluated from z_* to ∞ , and $d_A(z_*)$ is the comoving distance to last scattering surface:

$$d_A(z_*) = \int_0^{z_*} \frac{dz'}{H(z')} \quad (13)$$

The reported value for the Hubble constant by P15 is $H_0 = 67.8 \pm 0.9$ [16], which assumes a Λ CDM universe and is known to be in tension with AR16 at the 3.4σ level.

III. BACKGROUND EVOLUTION

Additionally to parameters in equation (3) we also investigate the constraints on the physical density of cold dark matter $\omega_c \equiv \Omega_c h^2$ and H_0 (or equivalently h), resulting in the set $\alpha = \{w_0, w_i, z_T, q, \omega_c, h\}$ and consider uniform priors on these: $h \in [0.5, 1]$, $\omega_c \in [0.001, 0.99]$, $w_0 \in [-1, 0]$, $w_i \in [-1, 0]$, $q \in [1, 10]$ and $z_T \in [0, 3]$. To determine the best-fitting values (BFV), we minimize the χ^2 goodness-of-fit estimator,

$$\chi^2 = (\mathbf{m} - \mathbf{d})^T \mathbf{C}^{-1} (\mathbf{m} - \mathbf{d}) \quad (14)$$

where \mathbf{m} are theoretical values for each observable (namely $r_{BAO}(z)$, H_0 , ω_c , θ_*) and \mathbf{d} the data. The

Data set	Redshift	$r_{BAO}(z)$
6dF	0.106 [27]	0.336 ± 0.015
SDSS DR7	0.15 [32]	0.2239 ± 0.0084
SDSS(R) DR7	0.35 [33]	0.1137 ± 0.0021
SDSS-III DR12	0.38 [30]	0.100 ± 0.0011
	0.61 [30]	0.0691 ± 0.0007
SDSS-III DR11	2.34 [35]	0.0320 ± 0.0013
	2.36 [34]	0.0329 ± 0.0009

TABLE I: $r_{BAO}(z)$ measurements used in this work. The ones corresponding to SDSS data were inverted from the published values of $D_V(z)/s_d$ and those corresponding to Ly α -F data were obtained from the reported quantities $D_A(z)/s_d$ and $D_H(z)/s_d$.

corresponding covariance matrix is represented by **C**.

The joint analysis of the different data sets is done by adding their respective χ^2 functions. Further details can be found in the Appendix A.

The reported value of Ω_m , $\rho_{DE} \equiv \Omega_{DE}h^2$ and $\rho_\Lambda \equiv \Omega_\Lambda h^2$ in tables summarizing our results was obtained by taking the BFV for ω_c and H_0 for each model, as well as the fixed value $\omega_b \equiv \Omega_b h^2 = 0.02225$ from P15 [16].

Results from this section are discussed below and summarized in table II, and in figures 2-3.

Local measurements (labeled model A in table II) point to a dynamical DE presenting a very late and abrupt transition ($z_T = 0.28$, $q = 9.97$) from an initial value $w_i = -0.99$ to a present value $w_0 = -0.91$. This behavior is portrayed in figure 2 and corresponds to the black dot-dashed curve. The value for H_0 holds in agreement with the reported measurement from AR16 used as prior for this calculation.

The dynamics for DE resulting from the use of BAO data and CMB reduced likelihood (outcome B, Table II) indicates the preference for a steep transition ($q = 9.8$) from the initial value $w_i = -0.77$ to the present value $w_0 = -0.92$ at a pivotal redshift $z_T = 0.63$. This corresponds to the dotted line in figure 2. The value for ω_c lies within the range imposed by CMB priors and the BFV for H_0 is lower, in agreement with P15 ([16]).

Model C in table II shows that a late time and smooth transition ($z_T=1.31$, $q = 1.5$) was preferred by data, with an initial value $w_i = 0$ to a present value $w_0 = -0.96$. The blue dashed line in 2 displays this particular dynamics. The amount of matter is very similar in DE and Λ CDM models (cases C and C_Λ), however we obtain a larger amount of DE $\rho_{DE} > \rho_\Lambda$ at present time and therefore a larger

H_0 . We see that the dynamics of DE allows to consistently fit the variables from CMB along with the local value of H_0 , since the inclusion of H_0 in model C only increased χ^2 by 0.2% compared to model B. However, from Table III we see that the addition of H_0 in Λ CDM model (B_Λ and C_Λ) severely penalizes the fit by increasing χ^2 by 19%, showing a tension in the value for H_0 from CMB and local measurements.

In this case, the DE density at early times is not negligible since it has $w_i = 0$. Figure 4 shows that its contribution at decoupling is of order $\Omega_{DE} = 10\%$, adding an extra component that behaves like dust ($\propto a^{-3}$) at large redshifts. The ratio of DE density to ordinary matter ($\omega_c + \omega_b$) is nearly constant from $z \gtrsim 5$ and has a value $\rho_{DE}(z_*)/\rho_m(z_*) = 0.16$ (Figure 4b). This changes several cosmological parameters, for instance the equivalence epoch, $a_{eq} \equiv \rho_r(a_{eq})/\rho_m(a_{eq})$, is smaller modifying the distance to the last scattering surface and the sound horizon at recombination. This is an interesting toy model worthwhile of further studies, and it will also impact CMB power spectrum and Large Scale Structure formation.

Having a non-negligible DE at earlier times, allows to put better constraints on its parameters: $\{w_i, q, z_T\}$.

A DE component which is non-negligible at early times as been studied in the literature and is known as Early Dark Energy (see for example [42]).

From both, table II and figure 3 we can draw the following general results. The value for w_0 is tightly constrained by observations. The scenario $w_0 = -1$ is included within 1σ error for all the cases. Generally speaking, for the outcomes where DE density becomes negligible at earlier times, we obtained weak or no constraints for the initial value of the EoS, w_i , the transition time, z_T , and the exponent q . In all outcomes, the values $q = 1$ and $z_T = 1$ are contained within 1σ of significance Figure 3 shows that w_i is highly degenerated with w_0 . The results for Λ CDM are summarized in table III.

IV. GROWTH OF PERTURBATIONS

We are interested in studying the effect that the transition featured by the EoS (3) has in the evolution of matter overdensities well inside the horizon in the matter-DE domination era. We do so by means of the following system of linearized equations:

Steep Equation of State for DE										
Alias	Data sets used	χ^2	w_0	w_i	q	z_T	ω_c	H_0	Ω_m	ρ_{DE}
A	BAO + H_0	9.59	$-0.92^{+0.15}_{-0.14}$	$-0.99(\leq -0.67)$	9.97	0.28	$0.1568^{+0.0244}_{-0.0208}$	$73.22^{+4.2}_{-4.1}$	$0.334^{+0.052}_{-0.044}$	0.3570
B	BAO+CMB	9.77	-0.92 ± 0.10	$-0.77 (\leq -0.27)$	9.8	$0.63(\geq 0.10)$	0.1195 ± 0.0031	67.80 ± 0.9	0.308 ± 0.008	0.3181
C	BAO+CMB+ H_0	9.79	$-0.96^{+0.22}_{-0.17}$	$0^{+0.04}_{-0.02}$	$1.5^{+1.3}_{-0.5}$	$1.31^{+1.42}_{-0.44}$	0.1195 ± 0.0034	73.26 ± 1.0	0.264 ± 0.008	0.3950

TABLE II: BFV and 1σ errors for the free parameters as result from the combined analysis of BAO data (table I) along with the local value of H_0 (9) and CMB priors (11). The value for Ω_m and $\rho_{DE} \equiv \Omega_{DE}h^2$ were derived as explained in the text.

Λ CDM						
Alias	Data sets used	χ^2	ω_c	H_0	Ω_m	ρ_Λ
A_Λ	BAO + H_0	10.05	0.1476 ± 0.0052	$73.56^{+2.0}_{-2.3}$	$0.3139^{+0.023}_{-0.026}$	0.3712
B_Λ	BAO + CMB	11.74	$0.1201^{+0.0088}_{-0.0099}$	70.20 ± 0.5	0.2889 ± 0.004	0.3504
C_Λ	BAO + CMB + H_0	13.98	0.1203 ± 0.0017	70.99 ± 0.5	0.2829 ± 0.004	0.3614

TABLE III: Similar to Table II but assuming $w = -1$ as equation of state. The reported parameters are ω_c and H_0 . The value for Ω_m and $\rho_\Lambda \equiv \Omega_\Lambda h^2$ were derived as explained in the text.

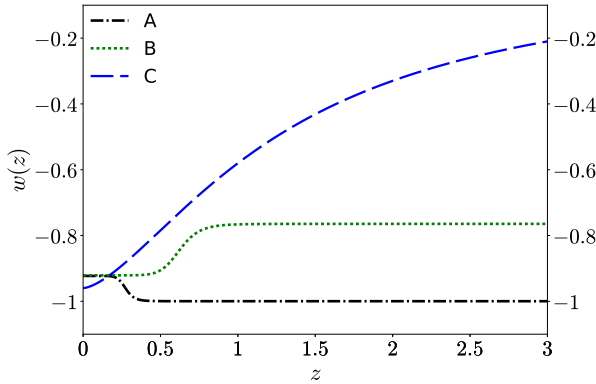


FIG. 2: Evolution of the EoS $w(z)$ in equation (3) according to the best fit values reported in Table II.

$$a^2 \delta_m''(a) + a \frac{3}{2} [1 - w(a)\Omega_{DE}(a)] \delta_m'(a) - \frac{3}{2} [\Omega_m(a)\delta_m(a) + \Omega_{DE}(a)\delta_{DE}(a)] = 0 \quad (15a)$$

$$a^2 \delta_{DE}''(a) + a \frac{3}{2} [1 - w(a)\Omega_{DE}(a)] \delta_{DE}'(a) + \left(\frac{c_s^2 k^2}{a^2 H^2(a)} - \frac{3}{2} \Omega_{DE}(a) \right) \delta_{DE}(a) - \frac{3}{2} \Omega_m(a)\delta_m(a) = 0, \quad (15b)$$

where $\delta_m \equiv \frac{\delta \rho_m}{\rho_m}$ and $\delta_{DE} \equiv \frac{\delta \rho_{DE}}{\rho_{DE}}$ represent the matter and DE density contrasts, respectively; $w(a)$ is the equation of state (3) as function of scale factor, Ω_{DE} and Ω_m are the DE and matter fractional den-

sities, $H(a)$, the Hubble function and k the Fourier wave number.

The term c_s^2 in equation (15b) represents the speed of sound for the DE. We can split it as the sum of an adiabatic contribution and an *effective* or *non-adiabatic* part:

$$c_s^2 \equiv \frac{\delta p}{\delta \rho} = c_{ad}^2 + c_{eff}^2. \quad (16)$$

c_{ad}^2 stands for the adiabatic speed of sound, defined as

$$c_{ad}^2 \equiv \frac{dP}{d\rho} = w(a) - \frac{aw'(a)}{3(1+w(a))} \quad (17)$$

which depends solely on the equation of state for the DE fluid and its derivative, whereas c_{eff}^2 represents the non-adiabatic contribution to the speed of sound. We model it as a constant and take some values, $c_{eff}^2 = 0, 1/3, 1$.

Figure 5 shows the effect a transition in the EoS has in c_{ad}^2 . We note that the greater the value for q , the sharper the bump in the adiabatic speed of sound. For this part of the analysis we take the values for $\{w_0, w_i, q, z_T\}$ as those resulting from A in Table II.

Adiabatic initial conditions were assumed and the value for δ_m was fixed to be $\delta_m(a_{ini}) = 10^{-5}$ at the time of entrance for the k-mode into the horizon, whose value was chosen to be $k = 0.01 Mpc^{-1}$.

Figure 6 displays the solution δ_m from equation (15) for an DE EoS modeled by result A (table II) and $c_{eff}^2 = 0, \frac{1}{3}, 1$. We note that the effect

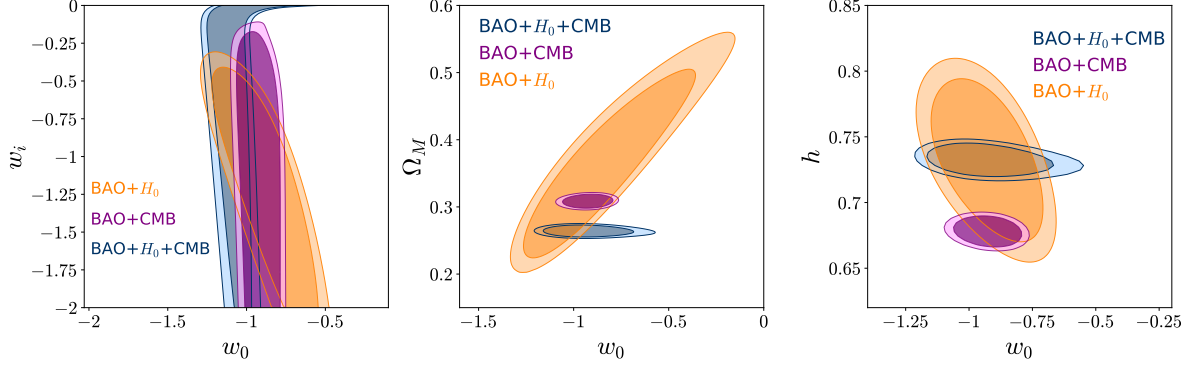
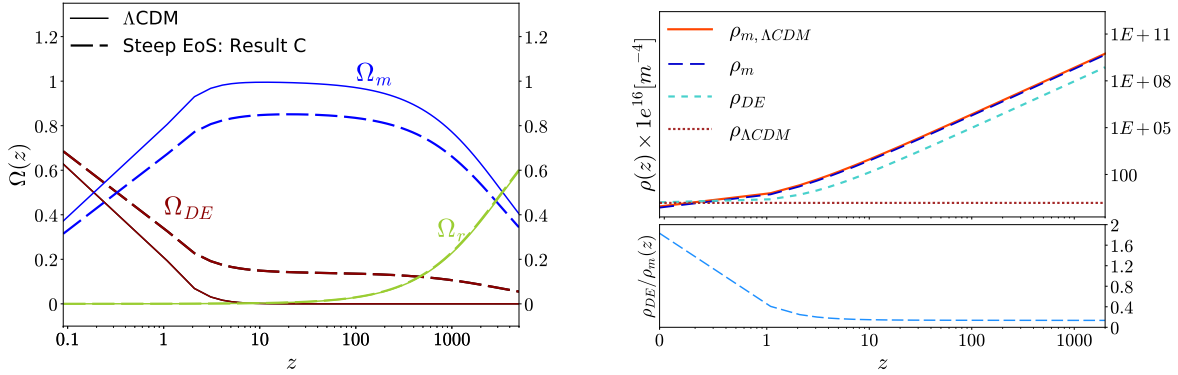


FIG. 3: Contour plots displaying the 1σ and 2σ confidence levels for the data sets presented in Table II on w_0 - w_i (left), w_0 - Ω_M (center), and w_0 - h space (right).



(a) Evolution of $\Omega_{DE}(z)$ (red), $\Omega_m(z)$ (blue) and $\Omega_r(z)$ (green) for a Cosmological Constant solution (solid line) and for DE (dashed line) analysis.

(b) Matter density for DE (long-dashed) and for Λ CDM (solid line), along with DE density (dashed line) and ρ_Λ (dotted line). Bottom panel: the ratio of DE density to ordinary matter (CDM and baryons)

FIG. 4: Comparison of DE following the dynamics resulting from BAO+ H_0 +CMB analysis (result C) and for Λ CDM.

of c_{eff}^2 is to reduce the magnitude in the growth of δ_m , keeping the shape the same. It is also notorious that the evolution of δ_m becomes very non-linear when solved coupled to δ_{DE} , due to the term $\left(\frac{c_s^2 k^2}{a^2 H^2(a)} - \frac{3}{2}\Omega_{DE}(a)\right)\delta_{DE}(a)$ in equation (15b).

The transition performed in the model A occurs at $z_T = 0.28$ with an steepness given by $q = 9.97$. The corresponding time of transition, $a_T = 1/(1+z_T) = 0.78$, is marked by a blue dashed vertical line in figures 6, 7, and 8.

In figure 7 we analyze in more detail the effect of a steep transition. We fix $c_{eff}^2 = 0$ to focus on the effect of c_{ad}^2 only (displayed in figure 5). For comparison we take the CPL with the same values for w_0 and w_i as in Result A and we take the ratio of both solutions. The result is displayed in the lower

panel of figure 7. We note the difference between $q = 1$ and $q = 9.8$ at the transition time, a_T , as a sudden increase during the transition.

Figure 8 shows the normalized growth function $D_m(a) \equiv \frac{\delta_m(a)}{\delta_m(a_0)}$ to the present value for the same models as in figure 7. The bottom panel shows the ratio to Λ CDM instead.

It is customary to take $\delta_{DE} = 0$. In such case, the system of equations (15) reduces to:

$$a^2 \delta_m'' + a \frac{3}{2} (1 - w(a)\Omega_{DE}(a)) \delta_m' - \frac{3}{2} \Omega_m(a) \delta_m = 0 \quad (18)$$

In figure 9 we show the solution to equation (18) for the case of a Λ CDM scenario, the best fit corresponding to Result A in table II, and its CPL limit (4). The bottom panel shows the relative difference from each model to Λ CDM, this is $\delta_m(z)/\delta_{m,\Lambda}(z)$,

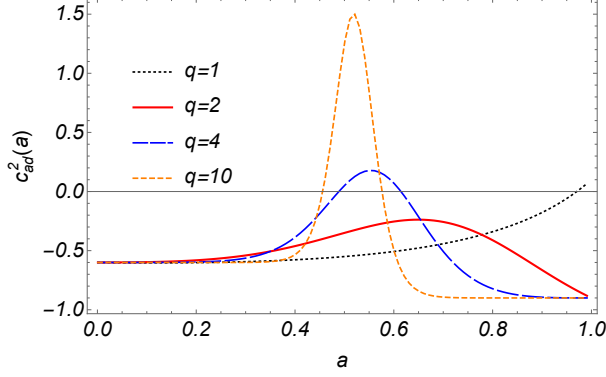


FIG. 5: Adiabatic sound speed c_{ad}^2 as function of scale factor assuming the EoS in equation (3) with $w_0 = -0.9$, $w_i = -0.6$, $z_T = 1$ and different values for the exponent: $q = 1$ (dotted black curve), $q = 2$ (dot-dashed red), $q = 4$ (dashed blue) and $q = 10$ (solid orange line).

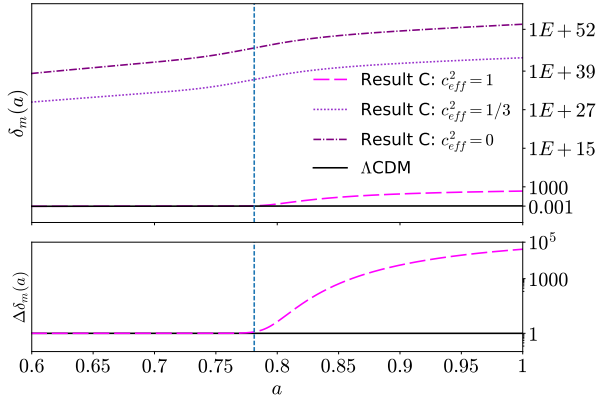


FIG. 6: (Upper panel) Solution for δ_m from the system of equations (15) taking values $c_{eff} = 1$ (dashed pink line), $c_{eff} = 1/3$ (violet dotted line), and $c_{eff} = 0$ (purple dot-dashed line) added to the adiabatic speed of sound, c_{ad}^2 (17). The dashed vertical line marks the transition time, a_T . (Lower panel) Ratio of solution with $c_{eff}^2 = 1$ to Λ CDM,

$$\Delta\delta_m \equiv \frac{\delta_m(a)}{\delta_{m,\Lambda CDM}}.$$

where $\delta_{m,\Lambda}(z)$ corresponds to the growth of matter contrast when we assume a Cosmological Constant solution. From $\delta_m(z)/\delta_{m,\Lambda}(z)$ we find differences from Λ CDM of around 1% for a k -mode of $k = 0.01 Mpc^{-1}$.

A deeper analysis on the impact of DE perturbations will be subject of a next paper [43].

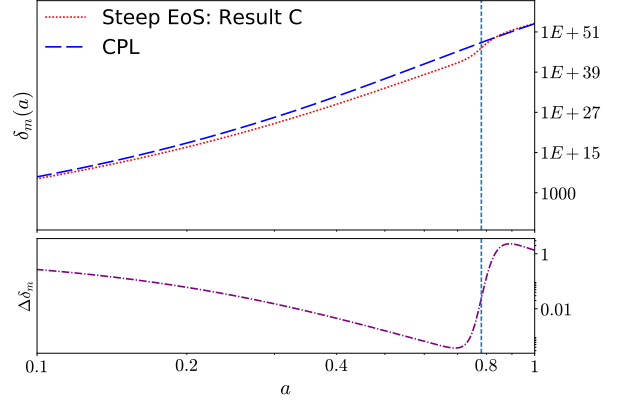


FIG. 7: (Upper panel) Growth of matter overdensities from the system of equations (15) taking $c_{eff}^2 = 0$ for the “BAO + H_0 ” model and its corresponding CPL limit, *i. e.*, $q = z_T = 1$. (Lower panel) Ratio of “BAO + H_0 ” solution to CPL

$$\text{limit, } \Delta\delta_m \equiv \frac{\delta_m(a)}{\delta_{m,CPL}}$$

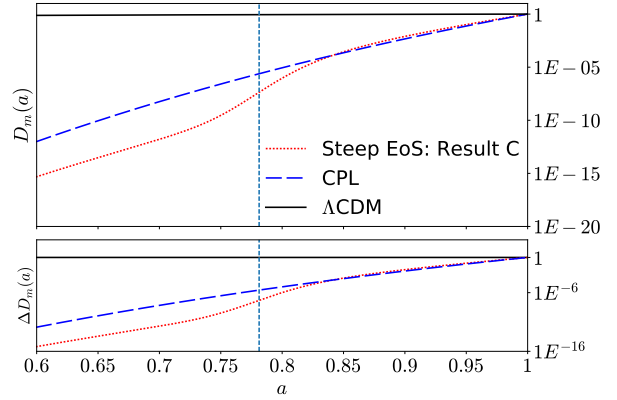


FIG. 8: (Upper panel) Same as in figure 7 but displaying the growth function normalized to the present day. (Lower panel) Ratio of “BAO + H_0 ” and CPL solutions to Λ CDM scenario,

$$\Delta D_m \equiv \frac{D_m}{D_{m,\Lambda CDM}}.$$

V. SUMMARY AND CONCLUSIONS

We presented a parametrization for the EoS of DE and found the constraints deduced by using BAO measurements contained in Table I combined with the latest local determination of Hubble constant ([37]). Additionally we used the compressed CMB likelihood from Planck ([16]), by means of the sound horizon at decoupling, θ_* , and $\omega_c h^2$.

The constraints for the free parameters, $\{w_0, w_i, q, z_t, \omega_c, H_0\}$, and their 68% errors resulting from the combined analysis of the datasets

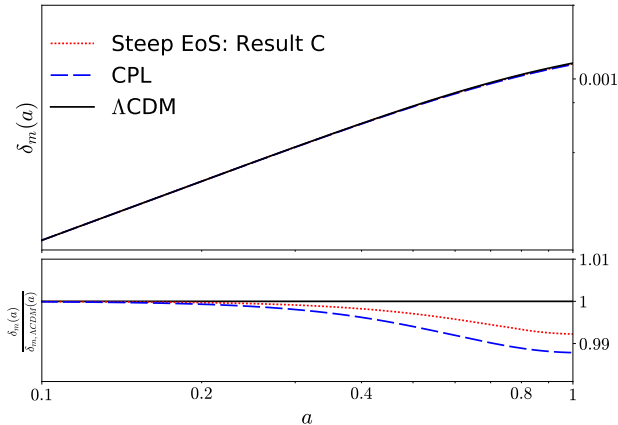


FIG. 9: (Upper panel) Growth of matter overdensity taking $\delta_{DE} = 0$ and the model “BAO+ H_0 ” as DE EoS. The CPL limit, (dashed blue line) and Λ CDM (solid black line) are also shown. (Lower panel) Ratio of CLP and “BAO+ H_0 ” solutions to Λ CDM: $\delta_m(a)/\delta_{m,LCDM}(a)$.

were obtained.

Our results show that a dynamical DE is favored by data and that a steep transition is preferred by local measurements, *i.e.* BAO and H_0 , and by BAO with CMB Planck observables (figure 2).

Whereas for a Λ CDM model, the tension between the local determination of H_0 ([37]) and the value derived from Planck ([16]) remains (table III), we find that it is possible to simultaneously conciliate the observations from BAO, H_0 and CMB in a single model (table II) by means of a dynamical Dark Energy.

For the perturbative analysis it was shown that the feature from the shape of c_{ad} due to the particular form of the EoS got imprinted in the evolution of δ_m . We modeled the speed of sound splitting it into an adiabatic contribution and an effective term, $c_s^2 = c_{ad}^2 + c_{eff}^2$, where c_{eff}^2 encapsulates the physics beyond the EoS of the dark fluid. The addition of this effective term did not erase the features from the bump in the adiabatic speed of sound but suppresses the exponential evolution of the over-densities by several orders of magnitude. This should be studied in detail and will be subject to discussion in a future paper [43].

The solution $\delta_{DE} = 0$ is only exact for the case of a cosmological constant. To be consistent we need to take DE perturbations into account. The solution to (15) with c_s^2 taken as the adiabatic contribution (17) for the model “BAO+ H_0 ” reported in table II was shown in figure 8. From this we saw that if we take $c_s^2 = c_{ad}$, the solutions were highly unstable and became non-linear extremely fast during the evolution

of over-densities.

To summarize, the study of dynamics of Dark Energy is a matter of profound implications for our understanding of the Universe and its physical laws. Although the measurements from CMB are the most precise data sets in Cosmology, the best way to analyze the properties of DE comes from the low redshift regime, where the BAO feature is the most robust cosmic ruler. In this work we have contributed towards that direction, and we have presented the constraints for a dynamical DE model coming from the analysis of BAO distance measurements combined with the most recent H_0 determination and CMB information.

Acknowledgments

We acknowledge financial support from DGAPA-PAPIIT IN101415 and Conacyt Fronteras de la Ciencia 281 projects. MJ thanks Conacyt for financial support and to the attendees of MACSS for helpful discussions.

A. Appendix

For the BAO measurements we use the χ^2 function defined as

$$\chi_{BAO}^2 = \mathbf{y}_{BAO}^T \mathbf{C}_{BAO}^{-1} \mathbf{y}_{BAO}, \quad (\text{A1})$$

where $\mathbf{y}_{BAO} \equiv r_{BAO}^{Th}(\alpha|z_i) - r_{BAO}^{Obs}(z_i)$ is the difference between theoretical prediction for $r_{BAO}(z)$ according to (5) and the values listed in table I, and \mathbf{C}_{BAO}^{-1} is the inverse of the covariance matrix containing the observational errors for the measurements. Since the data points used in this work are not correlated we have a diagonal matrix whose elements are the square-root of the errors reported in table I.

Additionally to BAO data we make use of the local determination of H_0 by means of

$$\chi_{H_0}^2 = \frac{[H(\alpha|z=0) - H_0^{Obs}]^2}{\sigma_{H_0}^2} \quad (\text{A2})$$

where $H(\alpha|z=0)$ is the Hubble function (1) evaluated in $z=0$ taking the model described by α and $H_0^{Obs} = 73.24 km \cdot s^{-1} Mpc^{-1}$ and $\sigma_{H_0} = 1.74 km \cdot s^{-1} Mpc^{-1}$, according to the primary fit obtained by A. Riess *et al.* in [37].

Finally, for the CMB, we use the determination of θ_* and ω_c , made by the Planck Collaboration (P. A. R. Ade *et al.* 2015, [16]). In particular we use *Planck TT + TE + EE + low P* values from

the table 4 of [16] with the covariance matrix displayed in (11). With this matrix we can build the

χ_{CMB}^2 function:

$$\chi_{CMB}^2 = \mathbf{y}_{CMB}^T \mathbf{C}_{CMB}^{-1} \mathbf{y}_{CMB} \quad (\text{A3})$$

where \mathbf{y}_{CMB} is the corresponding data vector defined as $\mathbf{y}_{CMB} = [\omega_c^{Th} - \omega_c^{Planck}, \theta_*(\alpha)^{Th} - \theta_*^{Planck}]^T$, and \mathbf{C}_{CMB}^{-1} is the inverse of matrix (11).

-
- [1] Steven Weinberg. The cosmological constant problem. *Rev. Mod. Phys.*, 61:1–23, Jan 1989.
- [2] Varun Sahni. The Cosmological constant problem and quintessence. *Class. Quant. Grav.*, 19:3435–3448, 2002.
- [3] Michael Doran and Georg Robbers. Early dark energy cosmologies. *JCAP*, 0606:026, 2006.
- [4] D. Rubin et al. Looking Beyond Lambda with the Union Supernova Compilation. *Astrophys. J.*, 695:391–403, 2009.
- [5] J. Sollerman, E. Mörtzell, T. M. Davis, M. Blomqvist, B. Bassett, A. C. Becker, D. Cinabro, A. V. Filippenko, R. J. Foley, J. Frieman, P. Garnavich, H. Lampeitl, J. Marriner, R. Miquel, R. C. Nichol, M. W. Richmond, M. Sako, D. P. Schneider, M. Smith, J. T. Vanderplas, and J. C. Wheeler. First-Year Sloan Digital Sky Survey-II (SDSS-II) Supernova Results: Constraints on Nonstandard Cosmological Models. *Astrophys. J.*, 703:1374–1385, October 2009.
- [6] M. J. Mortonson, W. Hu, and D. Huterer. Testable dark energy predictions from current data. *Phys. Rev. D*, 81(6):063007, March 2010.
- [7] Steen Hannestad and Edvard Mortsell. Cosmological constraints on the dark energy equation of state and its evolution. *JCAP*, 0409:001, 2004.
- [8] H. K. Jassal, J. S. Bagla, and T. Padmanabhan. WMAP constraints on low redshift evolution of dark energy. *Mon. Not. Roy. Astron. Soc.*, 356:L11–L16, 2005.
- [9] Jing-Zhe Ma and Xin Zhang. Probing the dynamics of dark energy with novel parametrizations. *Phys. Lett.*, B699:233–238, 2011.
- [10] Dragan Huterer and Michael S. Turner. Probing the dark energy: Methods and strategies. *Phys. Rev.*, D64:123527, 2001.
- [11] Jochen Weller and Andreas Albrecht. Future supernovae observations as a probe of dark energy. *Phys. Rev.*, D65:103512, 2002.
- [12] Zhiqi Huang, J. Richard Bond, and Lev Kofman. Parameterizing and Measuring Dark Energy Trajectories from Late-Inflatons. *Astrophys. J.*, 726:64, 2011.
- [13] Axel de la Macorra. Dark Energy Parametrization motivated by Scalar Field Dynamics. 2015.
- [14] Michel Chevallier and David Polarski. Accelerating universes with scaling dark matter. *Int. J. Mod. Phys.*, D10:213–224, 2001.
- [15] Eric V. Linder. Exploring the expansion history of the universe. *Phys. Rev. Lett.*, 90:091301, 2003.
- [16] P. A. R. Ade et al. Planck 2015 results. XIII. Cosmological parameters. 2015.
- [17] A. de la Macorra and G. Piccinelli. General scalar fields as quintessence. *Phys. Rev.*, D61:123503, 2000.
- [18] Kyle S. Dawson et al. The SDSS-IV extended Baryon Oscillation Spectroscopic Survey: Overview and Early Data. *Astron. J.*, 151:44, 2016.
- [19] T. Abbott et al. The dark energy survey. 2005.
- [20] Michael Levi et al. The DESI Experiment, a whitepaper for Snowmass 2013. 2013.
- [21] Amir Aghamousa et al. The DESI Experiment Part I: Science, Targeting, and Survey Design. 2016.
- [22] Amir Aghamousa et al. The DESI Experiment Part II: Instrument Design. 2016.
- [23] R. Laureijs, J. Amiaux, S. Arduini, J. . Auguères, J. Brinchmann, R. Cole, M. Cropper, C. Dabin, L. Duvet, A. Ealet, and et al. Euclid Definition Study Report. *arXiv:1110.3193*, October 2011.
- [24] LSST Science Collaboration, P. A. Abell, J. Allison, S. F. Anderson, J. R. Andrew, J. R. P. Angel, L. Armus, D. Arnett, S. J. Asztalos, T. S. Axelrod, and et al. LSST Science Book, Version 2.0. *ArXiv e-prints*, December 2009.
- [25] Matthew Colless et al. The 2dF Galaxy Redshift Survey: Final data release. 2003.
- [26] Daniel J. Eisenstein et al. Detection of the baryon acoustic peak in the large-scale correlation function of SDSS luminous red galaxies. *Astrophys. J.*, 633:560–574, 2005.
- [27] F. Beutler, C. Blake, M. Colless, D. H. Jones, L. Staveley-Smith, L. Campbell, Q. Parker, W. Saunders, and F. Watson. The 6dF Galaxy Survey: baryon acoustic oscillations and the local Hubble constant. *MNRAS*, 416:3017–3032, October 2011.
- [28] Eyal A. Kazin et al. The WiggleZ Dark Energy Survey: improved distance measurements to $z = 1$ with reconstruction of the baryonic acoustic feature. *Mon. Not. Roy. Astron. Soc.*, 441(4):3524–3542, 2014.
- [29] Lauren Anderson et al. The clustering of galaxies in the SDSS-III Baryon Oscillation Spectroscopic Survey: measuring D_A and H at $z = 0.57$ from the baryon acoustic peak in the Data Release 9 spectroscopic Galaxy sample. *Mon. Not. Roy. Astron. Soc.*, 439(1):83–101, 2014.

- [30] Shadab Alam et al. The clustering of galaxies in the completed SDSS-III Baryon Oscillation Spectroscopic Survey: cosmological analysis of the DR12 galaxy sample. *Submitted to: Mon. Not. Roy. Astron. Soc.*, 2016.
- [31] Bruce A. Bassett and Renee Hlozek. Baryon Acoustic Oscillations. 2009.
- [32] Ashley J. Ross, Lado Samushia, Cullan Howlett, Will J. Percival, Angela Burden, and Marc Manera. The clustering of the SDSS DR7 main Galaxy sample – I. A 4 per cent distance measure at $z = 0.15$. *Mon. Not. Roy. Astron. Soc.*, 449(1):835–847, 2015.
- [33] Nikhil Padmanabhan, Xiaoying Xu, Daniel J. Eisenstein, Richard Scalzo, Antonio J. Cuesta, Kushal T. Mehta, and Eyal Kazin. A 2 per cent distance to $z = 0.35$ by reconstructing baryon acoustic oscillations – i. methods and application to the sloan digital sky survey. *Monthly Notices of the Royal Astronomical Society*, 427(3):2132–2145, 2012.
- [34] Andreu Font-Ribera et al. Quasar-Lyman α Forest Cross-Correlation from BOSS DR11 : Baryon Acoustic Oscillations. *JCAP*, 1405:027, 2014.
- [35] Timothée Delubac et al. Baryon acoustic oscillations in the Lyman α Forest of BOSS DR11 quasars. *Astron. Astrophys.*, 574:A59, 2015.
- [36] Florian Beutler, Chris Blake, Jun Koda, Felipe Marin, Hee-Jong Seo, Antonio J. Cuesta, and Donald P. Schneider. The BOSS?WiggleZ overlap region ? I. Baryon acoustic oscillations. *Mon. Not. Roy. Astron. Soc.*, 455(3):3230–3248, 2016.
- [37] Adam G. Riess et al. A 2.4% determination of the local value of the hubble constant. *Astrophys. J.*, 826(1):56, 2016.
- [38] P. A. R. Ade et al. Planck 2015 results. XIV. Dark energy and modified gravity. *Astron. Astrophys.*, 594:A14, 2016.
- [39] Silvia Galli, Karim Benabed, François Bouchet, Jean-François Cardoso, Franz Elsner, Eric Hivon, Anna Mangilli, Simon Prunet, and Benjamin Wandelt. Cmb polarization can constrain cosmology better than cmb temperature. *Phys. Rev. D*, 90:063504, Sep 2014.
- [40] Yun Wang and Pia Mukherjee. Observational constraints on dark energy and cosmic curvature. *Phys. Rev. D*, 76:103533, Nov 2007.
- [41] Pia Mukherjee, Martin Kunz, David Parkinson, and Yun Wang. Planck priors for dark energy surveys. *Phys. Rev. D*, 78:083529, Oct 2008.
- [42] Eric V. Linder and Georg Robbers. Shifting the Universe: Early Dark Energy and Standard Rulers. *JCAP*, 0806:004, 2008.
- [43] Mariana Jaber and Axel de la Macorra. Dark energy perturbations. in preparation.